Electronic Supplementary Material (ESI) for Journal of Materials Chemistry C.

Supporting Information

An Excited-State Intramolecular Proton-Transfer Responsive Nanoscale MOF for the Dual Sensing of Water and Chromate Ions

Adrija Ghosh[a], Nivedita Sikdar[b] and Tapas Kumar Maji[a,b]*

[a]*New Chemistry Unit (NCU),* [b]*Chemistry and Physics of Material Unit (CPMU), School of Advanced Materials (SAMat), Jawaharlal Nehru Centre for Advanced Scientific Research, Jakkur, Bangalore-560064, India*

**Email: tmaji@jncasr.ac.in, www.jncasr.ac.in/tmaji; Tel: 91-8022082826*

Experimental Section:

Materials: All the reagents and solvents were used as obtained from commercial supplies without any further purification. 2,5-Dihydroxyterepthalic acid (DHT), 1,2-Di(4-pyridyl)ethylene (bpee), Dodecanoic acid (dda), Zinc nitrate hexahydrate ($Zn(NO_3)_2.H_2O$, and Potassium chromate (K_2CrO_4) were procured from Aldrich Chemical Co. Ltd. HPLC grade solvents were used for photophysical studies.

Physical Measurements:

Elemental analyses were performed in Thermo Scientific Flash 2000 CHN analyser. Thermal stability of the materials was analysed by Thermogravimetric analysis (TGA) using Mettler-Toledo TGA 850 under an inert atmosphere (N_2 flow rate = 50 mol min^{-1}) in the temperature range of 25-850°C at a heating rate of 5°C/min. Powder X-ray diffraction (PXRD) patterns were recorded on a Bruker D8 Discover instrument (40 kV, 30 mA) by using Cu-Kα radiation. Electronic absorption spectra were recorded on a Perkin Elmer Model Lambda 900 Spectrophotometer. Photoluminescence studies were carried out in a Fluorolog 3.21 spectrofluorometer (HORIBA Jobin-Yvon) instrument. The fluorescence decay profiles of the samples were recorded in a Horiba Delta Flex time-correlated single-photon counting (TCSPC). In order to measure the photoluminescence (PL) quantum yield values, 0.5 mg Zn-db MOF was dispersed in 1 mL solvent. The PL quantum yield was determined in solution state by an absolute method using a spectrofluorometer equipped with a 120 mm integrating sphere with a BENFLEC coated inner face (FLS1000 spectrometer Edinburgh Instruments). FTIR spectra of the compounds were recorded on a Bruker IFS 66v/S spectrophotometer using the KBr pellets in the region 4000−400 cm^{-1}. Inductively Coupled Plasma-Optical Emission Spectroscopy (ICP-OES) measurements were recorded on Perkin Elmer Optima 7000dv ICP-OES. N_2 adsorption isotherm at 77 K was recorded with the dehydrated sample using the Quantachrome Autosorb iQ analyser, wherein, 100 mg of the sample was degassed at 120°C at 1 bar vacuum for 10 hours before commencing measurements. Morphological studies were performed employing Lica-S440I Field Emission Scanning Electron Microscope (FE-SEM) with an accelerating voltage of 100 kV under high vacuum. Transmission Electron Microscopy (TEM) analysis was performed using JEOL JEM-3010 with an accelerating voltage of 300 kV.

Table S1: Tabulated representation of the coordination modulation method employed for synthesis.

Compound Name	Reactants				dda/Na_2H_2DHT (r)
	Na_2H_2DHT (mmol)	bpee (mmol)	$Zn(NO_3)_2.6H_2O$ (mmol)	dda (mmol)	
Zn-db	0.187	0.062	0.25	-	-
Zn-db-1	0.187	0.062	0.25	0.0625	0.33
Zn-db-2	0.187	0.062	0.25	0.125	0.66
Zn-db-3	0.187	0.062	0.25	0.25	1.33

Single crystal X-ray Diffraction:

X-ray single crystal structural data of **Zn-db** (CCDC 2114164) were collected on a Bruker Smart-CCD diffractometer equipped with a normal focus, 2.4 kW sealed tube X-ray source with graphite monochromated Mo-Kα radiation (λ = 0.71073 Å) operating at 50 kV and 30 mA. The program SAINT[1] was used for integration of diffraction profiles and absorption correction was made with SADABS[2] program. All the structures were solved by SIR 92[3] and refined by the full matrix least-squares method using SHELXL-97.[4] All the hydrogen atoms were fixed by HFIX and placed in ideal positions. Potential solvent accessible area or void space was calculated using the PLATON multipurpose crystallographic software.[5] All crystallographic and structure refinement data of **Zn-db** are summarized in Table S2. Selected bond lengths and angles for **Zn-db** are given in Tables S3 and S4. All calculations were carried out using SHELXL 97, PLATON, SHELXS 97 and WinGX system, Ver 1.70.01.[6] Solvent molecules have not been assigned.

Table S2: Crystal data and structure refinement parameters of **Zn-db**.

Parameters	Zn-db
Empirical formula	$C_{18}H_8NO_{10}Zn_2$
Formula weight	528.99
Crystal system	Monoclinic

Space group	*C*2/*c*
a, Å	20.631(5)
b, Å	25.846(5)
c, Å	14.114(5)
V, Å^3	6289.0(3)
Z	8
T, K	293
μ,mm^{-1}	1.562
D_{calcd},g/cm^3	1.117
F (000)	4056
Reflections [$I>2\sigma(I)$]	4354
Unique reflections	5593
Total reflections	55040
R_{int}	0.076
GOF on F^2	1.125
R_1[I>2σ(I)][a]	0.0687
R_w[all data][b]	0.0869
Δρ max/min [e Å^{-3}]	2.042, -0.77

[a]$R_1 = \sum||F_o|-|F_c||/\sum|F_o|$;[b]$R_w = [\sum\{w(F_o^2-F_c^2)^2\}/\sum\{w(F_o^2)^2\}]^{1/2}$

Table S3: Selected Bond Distances (Å) for **Zn-db**.

Bonds	**Bond lengths (Å)**	**Bonds**	**Bond lengths (Å)**
Zn1-O1	2.023(4)	Zn2-O3	1.921(3)
Zn1-N1	2.090(4)	Zn2-O6	1.956(4)
Zn1-O2	2.047(5)	Zn2-O7	2.004(5)
Zn1-O9	2.178(9)		

Symmetry code: a=-x,y,1/2-z

Table S4: Selected bond angles (°) for **Zn-db**.

Bonds	**Bond angles (°)**	**Bonds**	**Bond angles (°)**
O1-Zn1-N1	176.5(2)	O2-Zn1-O8	178.0(2)

O1-Zn1-O2	86.1(2)	O9-Zn1-O5	174.0(3)
O1-Zn1-O9	90.8(3)	O9-Zn1-O8	86.7(3)
O1-Zn1-O5	88.7(2)	O5-Zn1-O8	87.4(2)
O1-Zn1-O8	93.6(2)	O3-Zn2-O6	125.2(2)
N1-Zn1-O2	92.0(2)	O3-Zn2-O7	95.0(2)
N1-Zn1-O9	92.2(2)	O3-Zn2-O1	117.9(2)
N1-Zn1-O5	88.5(2)	O6-Zn2-O7	100.0(2)
N1-Zn1-O8	88.4(2)	O6-Zn2-O1	110.0(2)
O2-Zn1-O9	91.4(3)	O7-Zn2-O1	101.8(2)
O2-Zn1-O5	94.6(2)		

Symmetry code: a=-x,y,1/2-z

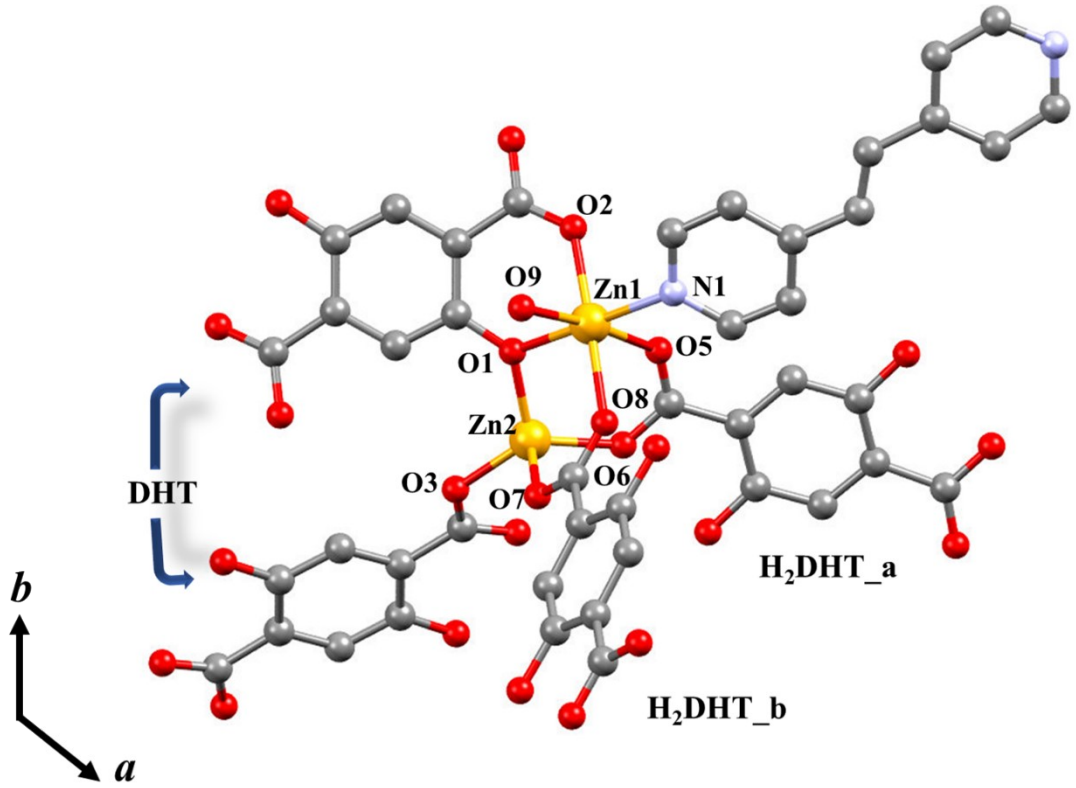

Fig. S1 Coordination environment of Zn1 and Zn2 in **Zn-db**.

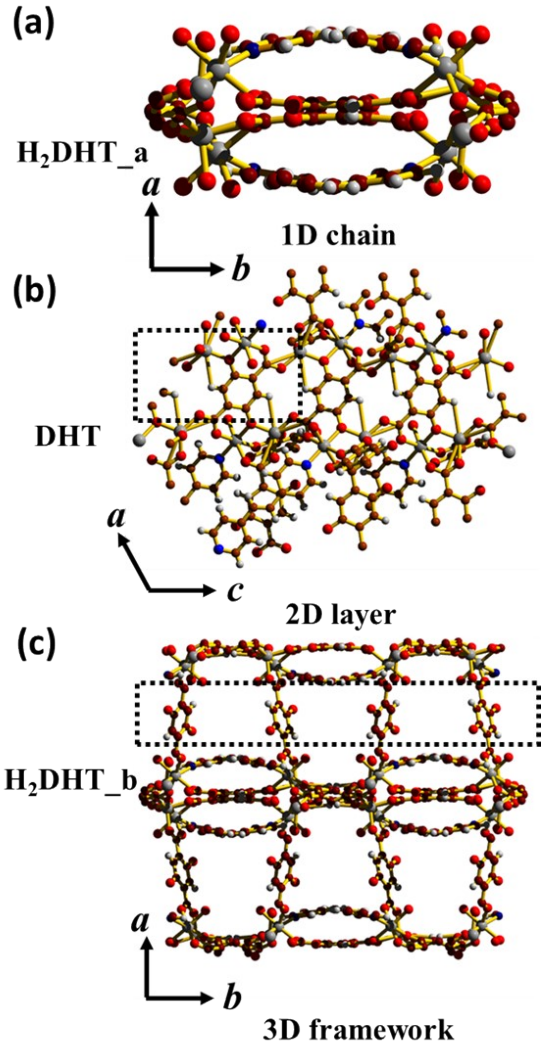

Fig. S2 View of the crystal structure of **Zn-db** along different crystallographic directions: **(a)** 1D coordination chain. **(b)** 2D layer along the *ac* plane. **(c)** 3D framework.

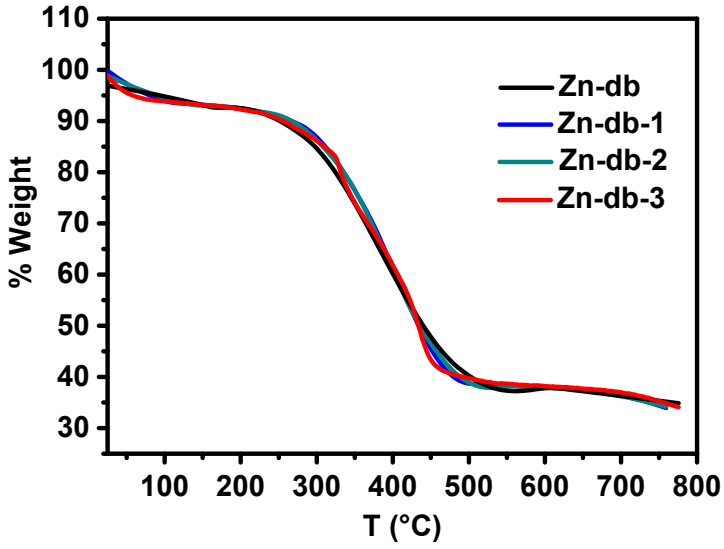

Fig. S3 TGA profiles for **Zn-db, Zn-db-1, Zn-db-2** and **Zn-db-3**.

Table S5: Summary of N_2 adsorption analysis of bulk Zn-db and its downsized analogues.

Sample	Zn-db	Zn-db-1	Zn-db-2	Zn-dn-3
N_2 uptake	7 m^3g^{-1}	11 m^3g^{-1}	57 m^3 g^{-1}	144 cm^3 g^{-1}
BET surface area	4 m^2g^{-1}	18 m^2 g^{-1}	66 m^2 g^{-1}	365 m^2 g^{-1}

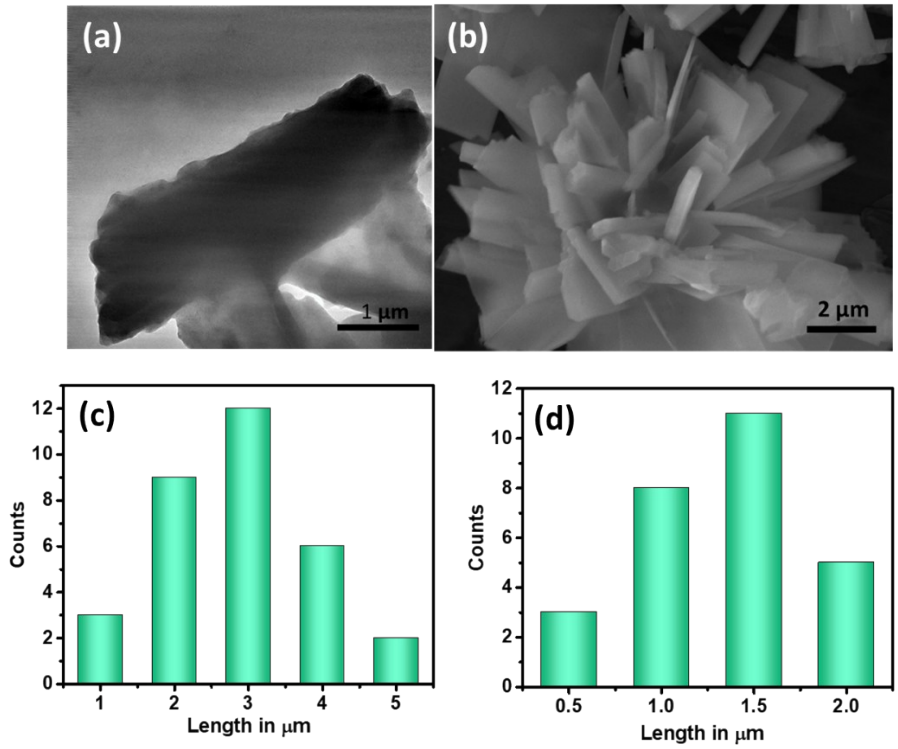

Fig. S4 (a) TEM image of **Zn-db-1**, **(b)** FESEM image of **Zn-db-1**, **(c)** Average length of mesosheets, **(d)** Average width of mesosheets.

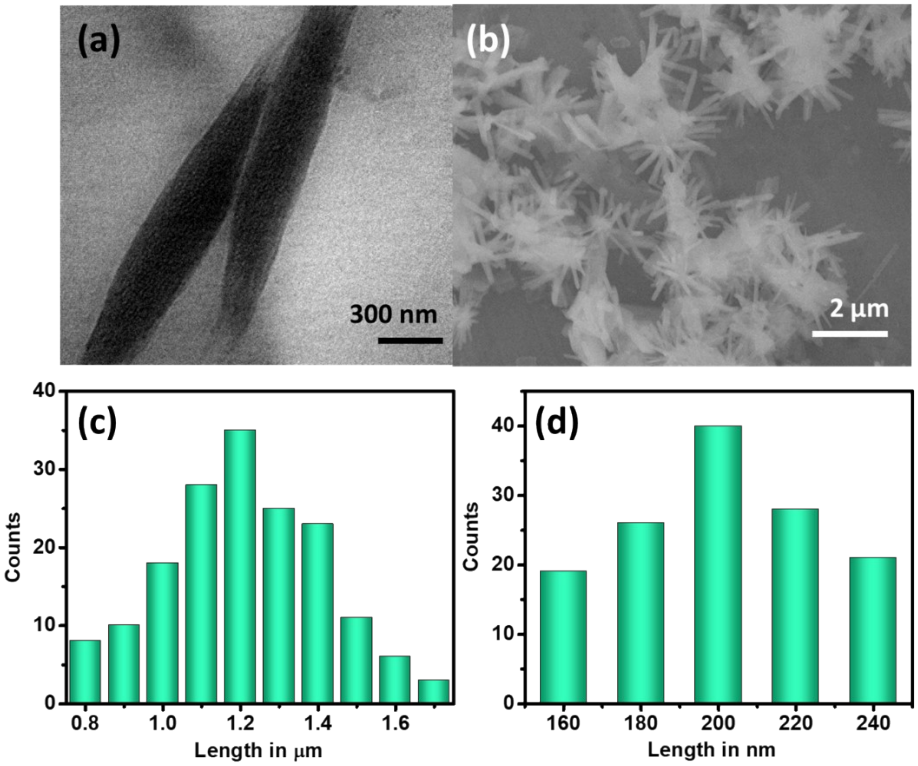

Fig. S5 (a) TEM image of **Zn-db-2**, **(b)** FESEM images of **Zn-db-2**, **(c)** Average length of nanorods, **(d)** Average diameters of nanorods.

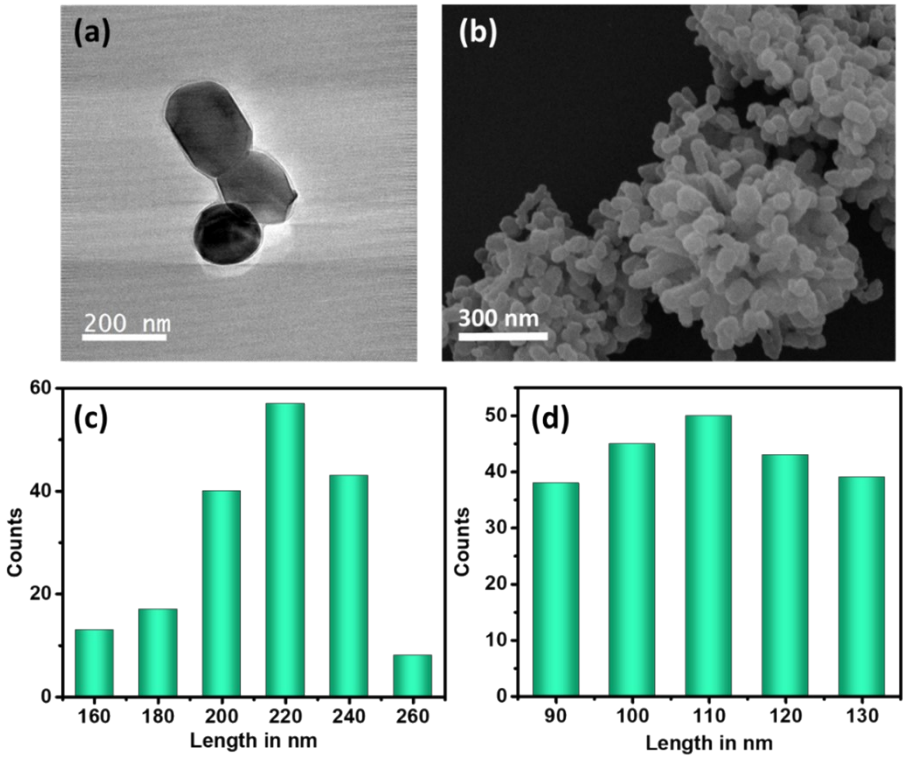

Fig. S6 (a) TEM images of **Zn-db-3**, **(b)** FESEM image of **Zn-db-3**, **(c)** Average length of nanoparticles along major axis, **(d)** Average length of nanoparticles along minor axis.

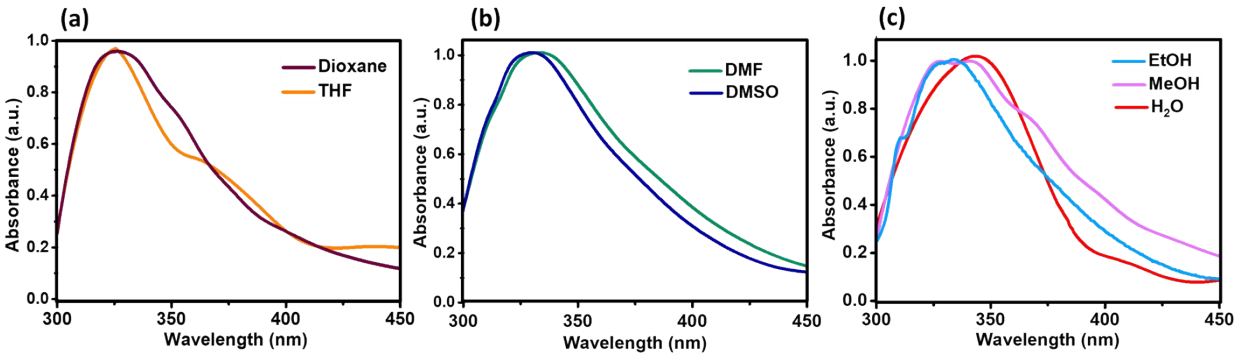

Fig. S7 Absorption spectra of **Zn-db-3** in **(a)** non-polar solvents, **(b)** polar aprotic solvents, **(c)** polar protic solvents.

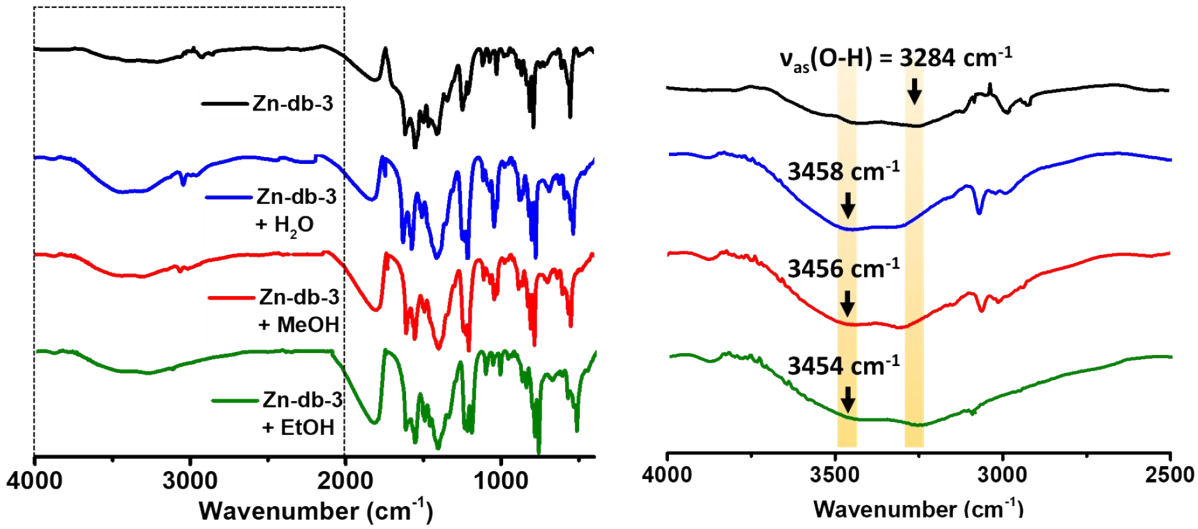

Fig. S8 FT-IR spectra of pristine dry **Zn-db-3** and **Zn-db-3** upon exposure to trace amounts of polar protic solvents (H_2O, MeOH, and EtOH).

Table S6. Summary of Time-resolved photoluminescence decay of **Zn-db-3** in different solvents.

Solvent	B_1	B_2	τ_1 (ns)	τ_2 (ns)	τ_{av} (ns)
THF	29.99%	70.01%	1.09	5.23	3.98
Dioxane	50.09%	49.91%	1.00	7.48	4.23
DMF	14.05%	85.95%	2.91	9.28	8.38
DMSO	11.93%	88.07%	2.64	9.29	8.49
MeOH	13.28%	86.72%	2.45	7.82	7.10
EtOH	29.20%	70.80%	2.18	9.01	7.01
H_2O	100%	-	4.53	-	4.53

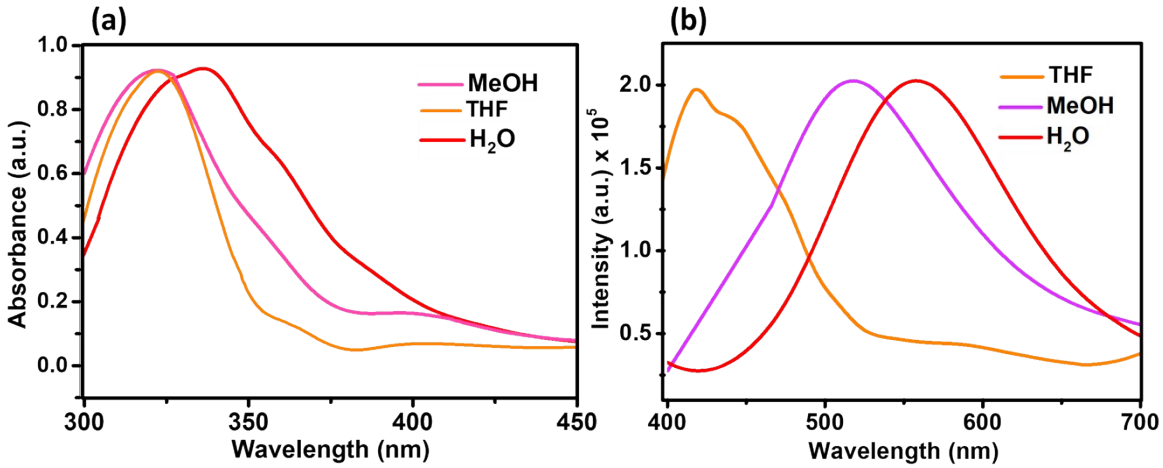

Fig. S9 (a) Absorption spectra of **H_4DHT** linker in different solvents. **(b)** Emission spectra of H_4**DHT** in different solvents.

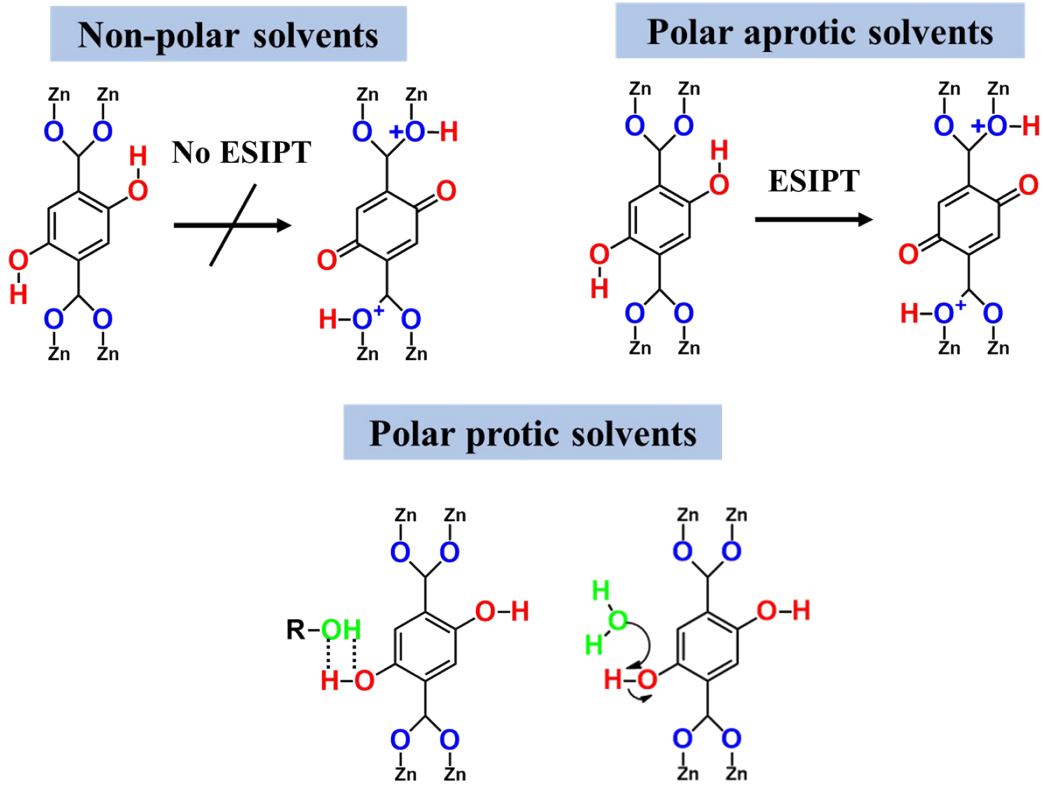

Fig. S10 Schematic representation of ESIPT in **Zn-db-3** in non-polar, polar aprotic, and polar protic solvents.

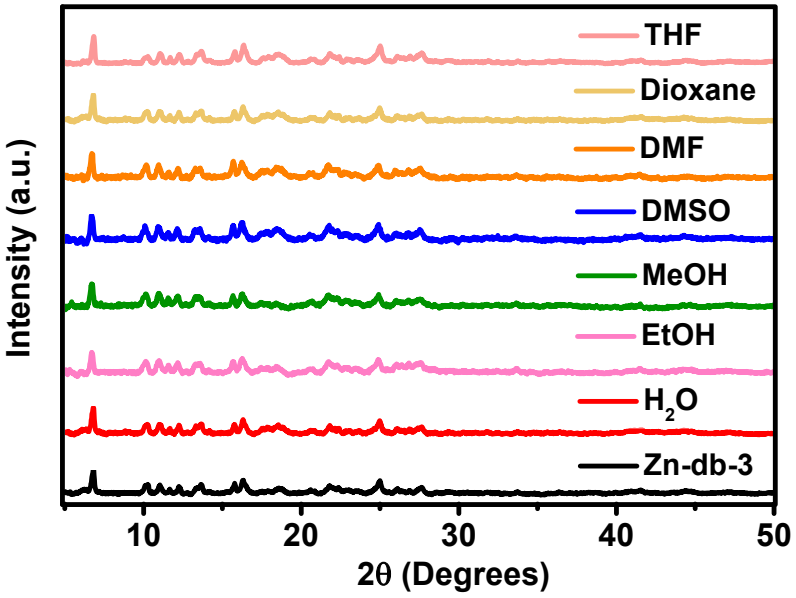

Fig. S11 PXRD patterns of **Zn-db-3** after immersion in different solvents.

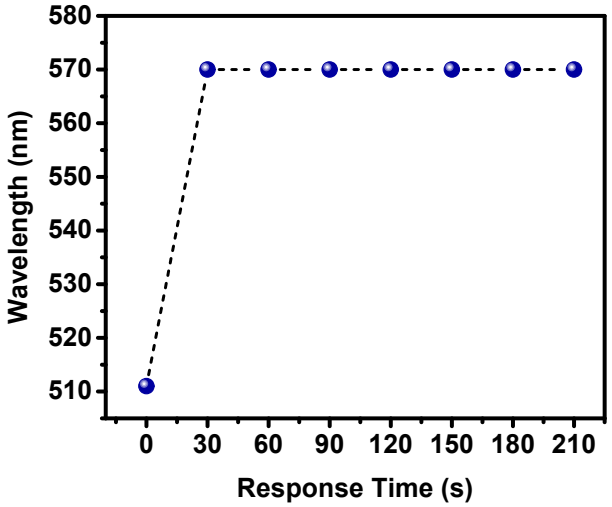

Fig. S12 Response time of **Zn-db-3** for the detection of 8% v/v H_2O in EtOH.

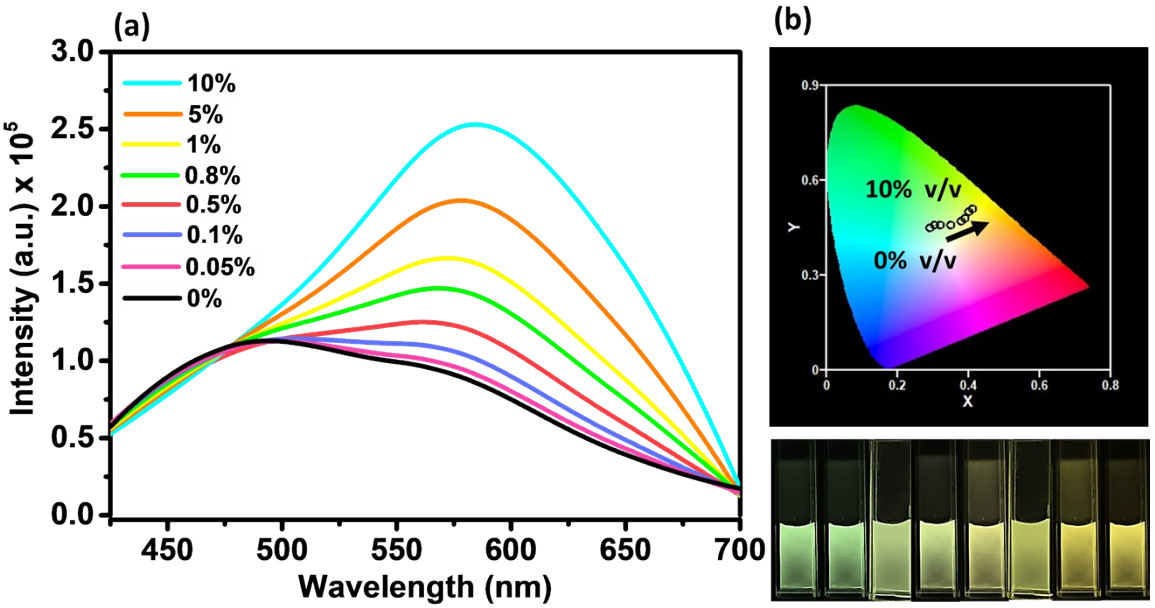

Fig. S13 (a) Enhanced emission intensity and shift observed upon addition of aliquots of H_2O to a dispersion of **Zn-db-3 in MeOH. (b)** CIE coordinates depicting the shift in emission and corresponding photographs taken under UV light.

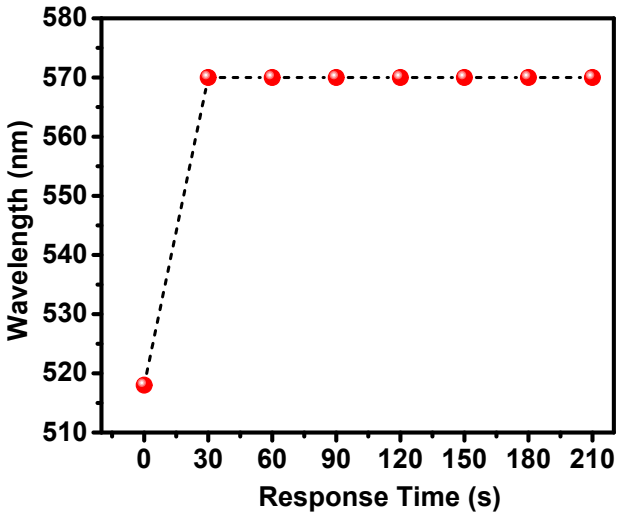

Fig. S14 Response time of **Zn-db-3** for the detection of 8% v/v H_2O in MeOH.

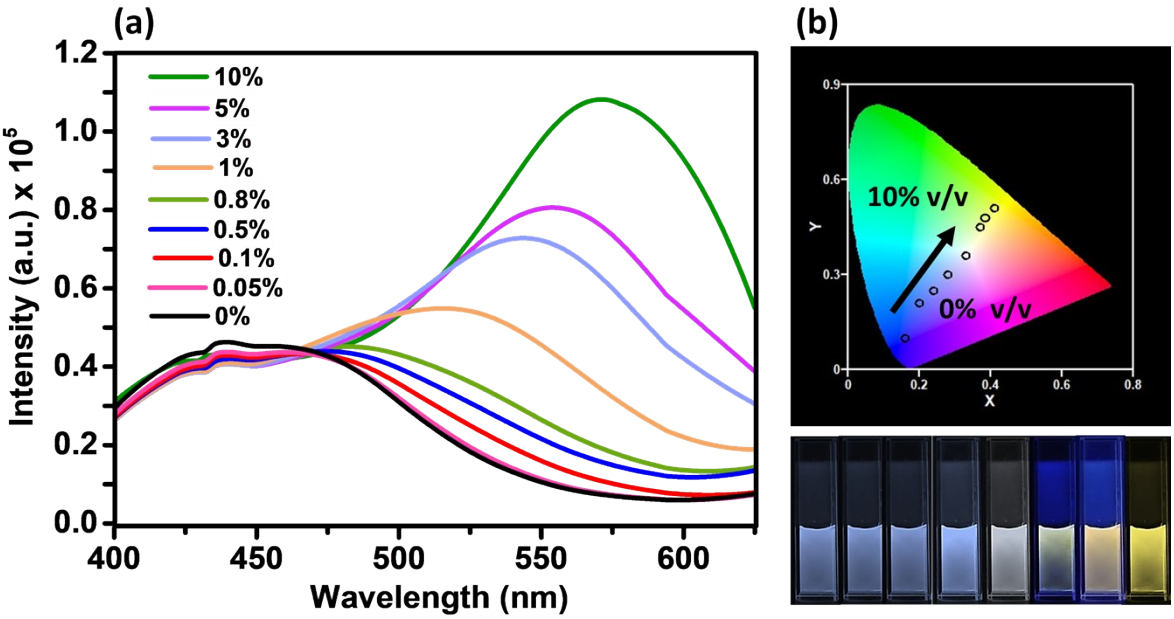

Fig. S15 (a) Enhanced emission intensity and shift observed upon addition of aliquots of H_2O to a dispersion of **Zn-db-3 in THF. (b)** CIE coordinates depicting the shift in emission and corresponding photographs taken under UV light.

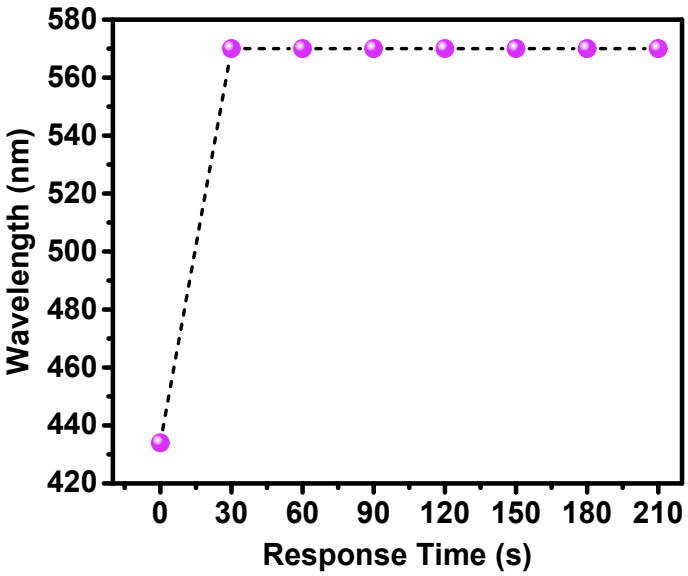

Fig. S16 Response time of **Zn-db-3** for the detection of 8% v/v H_2O in THF.

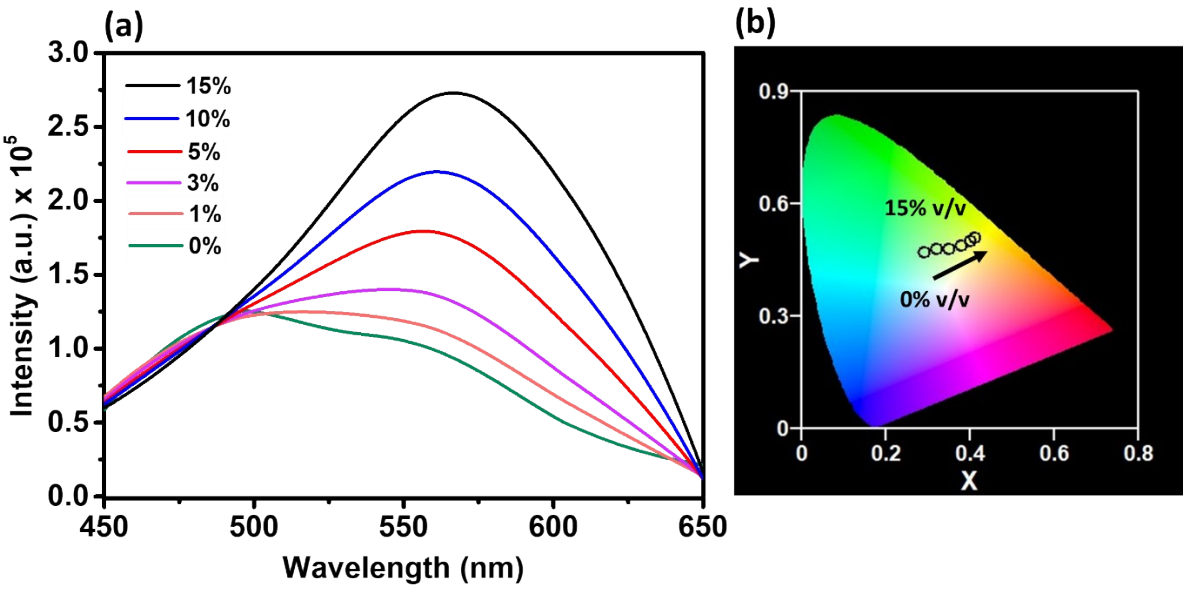

Fig. S17 (a) Enhanced emission intensity and shift observed upon addition of aliquots of H_2O to a dispersion of **Zn-db in EtOH. (b)** CIE coordinates depicting the shift in emission.

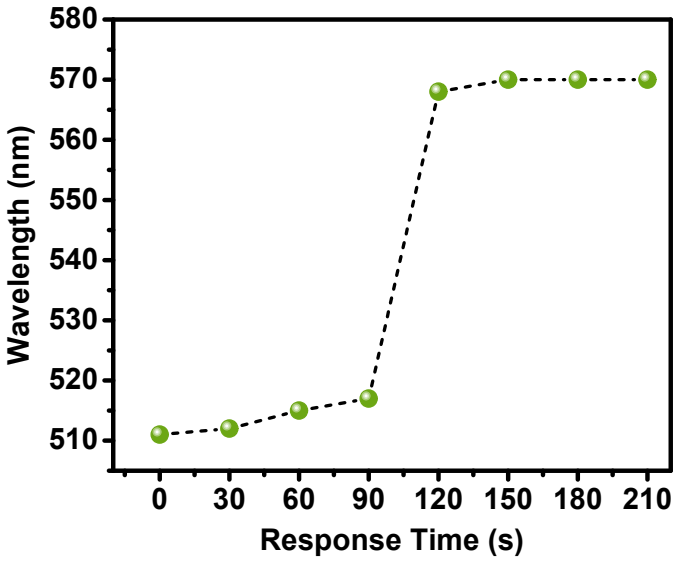

Fig. S18 Response time of **Zn-db** for the detection of 8% v/v H_2O in EtOH.

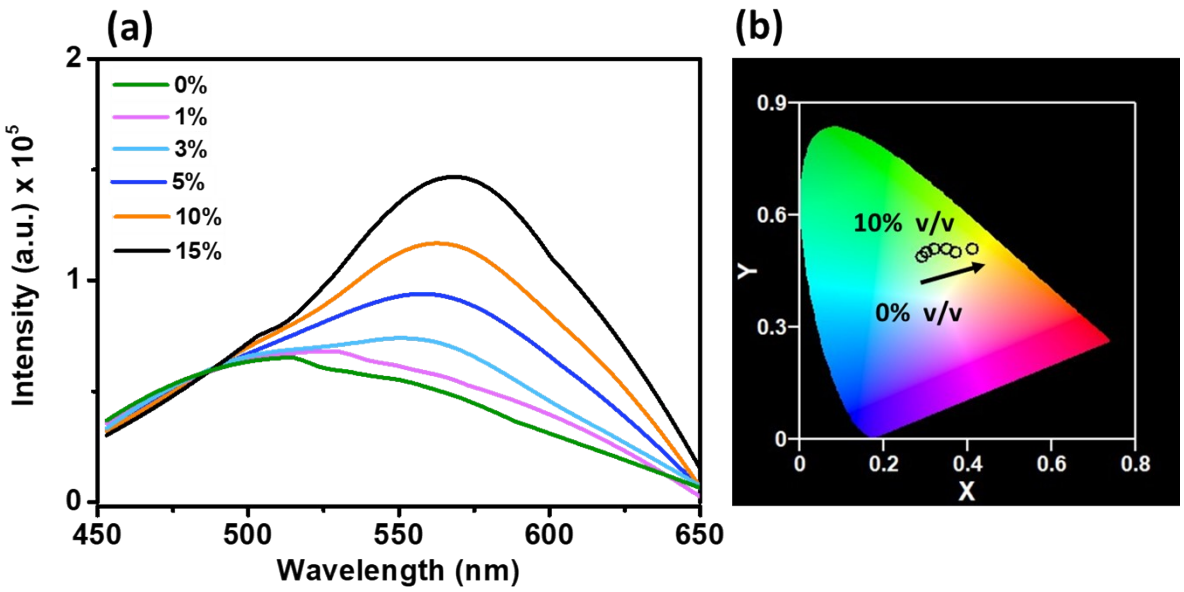

Fig. S19 (a) Enhanced emission intensity and shift observed upon addition of aliquots of H_2O to a solution of **H_4DHT** in EtOH (0.5 mg/mL). **(b)** CIE coordinates depicting the shift in emission.

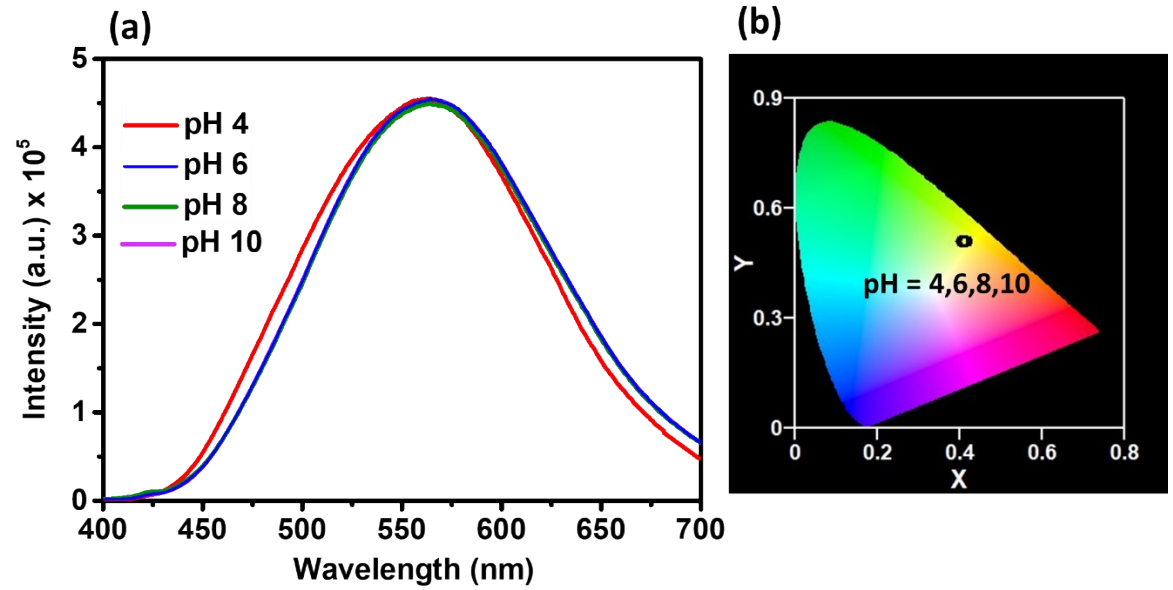

Fig. S20 (a) PL emission spectra recorded for **Zn-db-3** upon exposure to H_2O in the pH range of 4-10. **(b)** CIE coordinates depicting the shift in emission.

Table S7 Comparison of H_2O sensing performance of luminescent MOF materials

MOF	Media	LOD (% v/v)	Detection range	Detection Method	Response Time	Ref.

$Eu_{0.02}Dy_{0.18}$-MOF	Ethanol	0.1	0-0.3%	Turn-off	-	7
Tb^{3+}@p-CDs/MOF	DMF	0.33	0-30%	Turn-off	-	8
Eu^{3+}@UiO-66-NH_2-IM	Ethanol	0.05	0-2%	Turn-off	-	9
MOF@Fe_3O_4/SiO_2 composite	Hexane	0.03	0-10%	Turn-off		10
[Cd_2(4,5-idc)(2,5-tpt)(H_2O)$_4$]	DMF	0.25	0-50%	Shifted emission and turn-off	< 30s	11
LIFM-CL1-H_2O	Acetonitrile	0.05	0-1.3%	Shifted emission	-	12
AEMOF-1’	THF	-	0-5%	Shifted emission	60-120s	13
$Tb_{97.11}Eu_{2.89}$-L1	CH_3CN	0.04	0-2.5%	Turn-off	-	14
Zn-db-3	**Ethanol**	**0.05**	**0-15%**	**Shifted emission**	**< 30 s**	**This work**
	Methanol	**0.05**	**0-10%**	**Shifted emission**	**< 30 s**	
	THF	**0.05**	**0-10%**	**Shifted emission**	**< 30 s**	

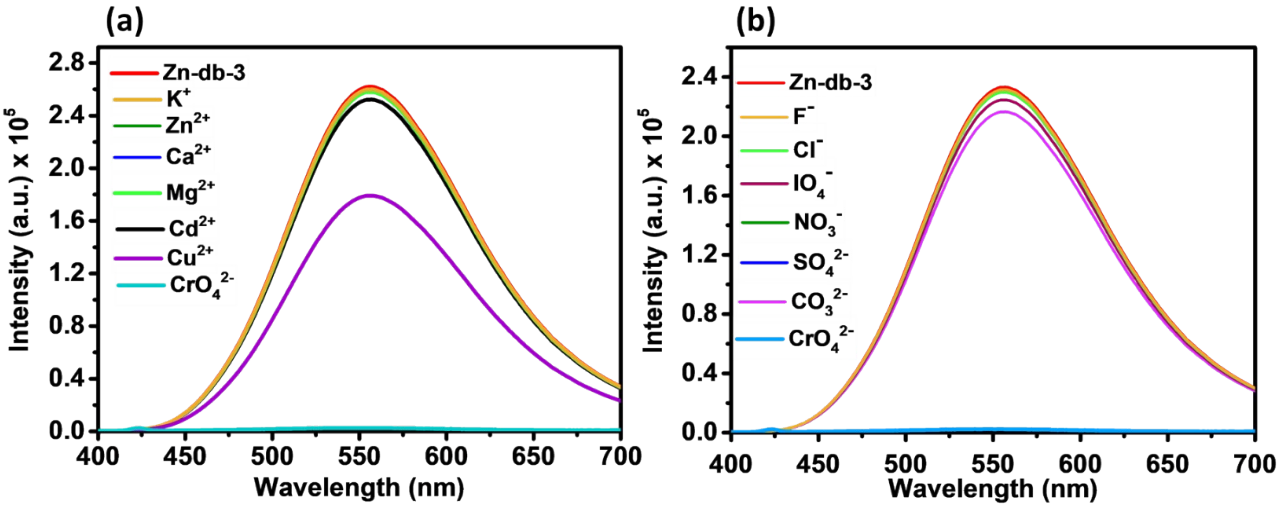

Fig.S21 Influence of competitive **(a)** cations and **(b)** anions upon the emission intensity of **Zn-db-3** dispersed in H_2O.

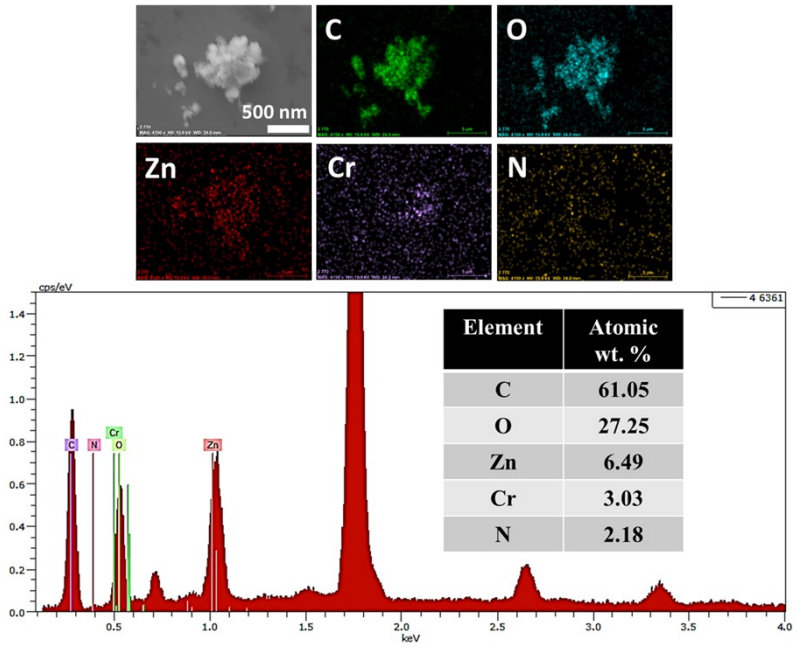

Fig. S22 FESEM and EDX analysis of **Cr^{6+}@Zn-db-3**

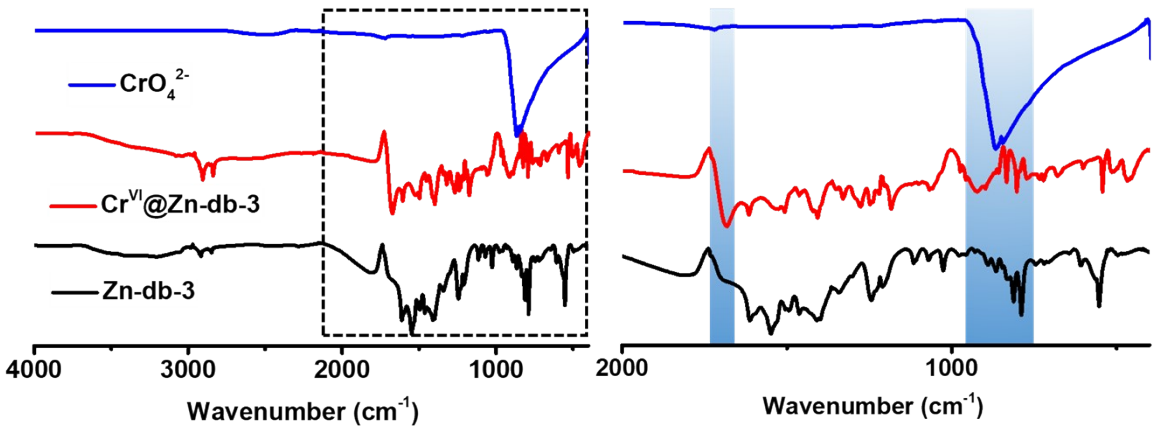

Fig. S23 FTIR spectra of **Zn-db-3**, **Cr^{6+}@Zn-db-3**, and **CrO_4^{2-}**

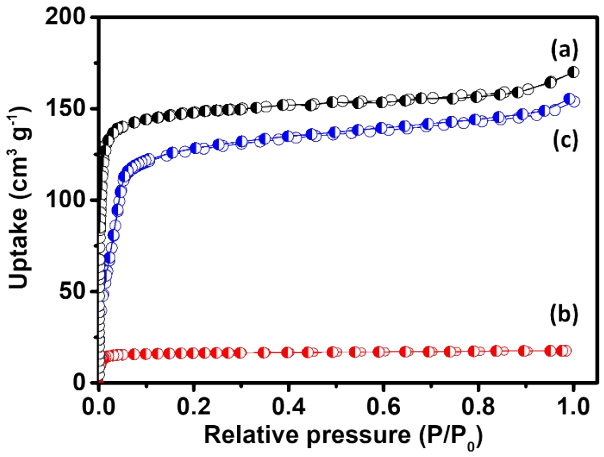

Fig. S24 N_2 adsorption isotherms recorded for **(a) Zn-db-3**, **(b) Cr^{6+}@Zn-db-3**, and **(c) Zn-db-3** recovered after the removal of CrO_4^{2-} ions(Unfilled circles represent the adsorption and the half-filled circles represent the desorption isotherm respectively).

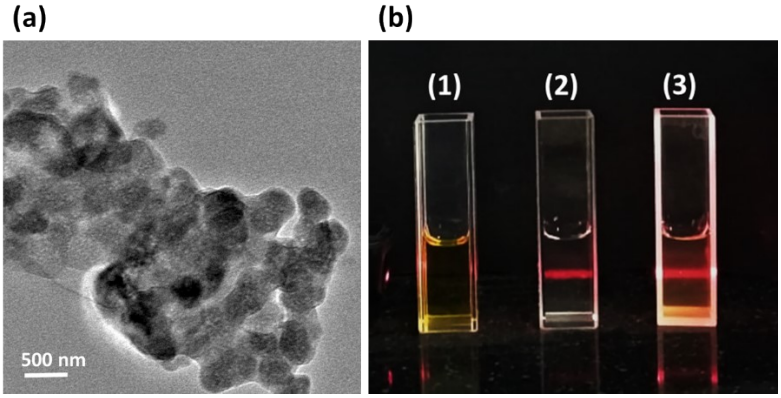

Fig. S25 (a) TEM image of **Cr^{6+}@Zn-db-3**. **(b)** Tyndall effect for an aqueous solution of **CrO_4^{2-}** ions (1), dispersion of **Zn-db-3** in H_2O (2) and a dispersion of **Cr^{6+}@Zn-db-3** in H_2O.

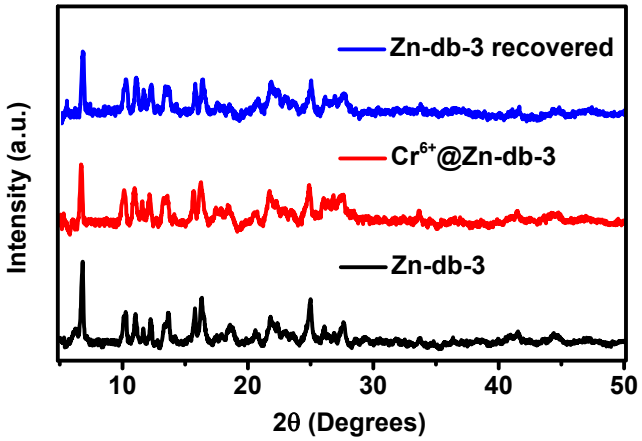

Fig. S26 PXRD patterns of **Zn-db-3**, **Cr^{6+}@Zn-db-3**, and **Zn-db-3** recovered after washing with H_2O.

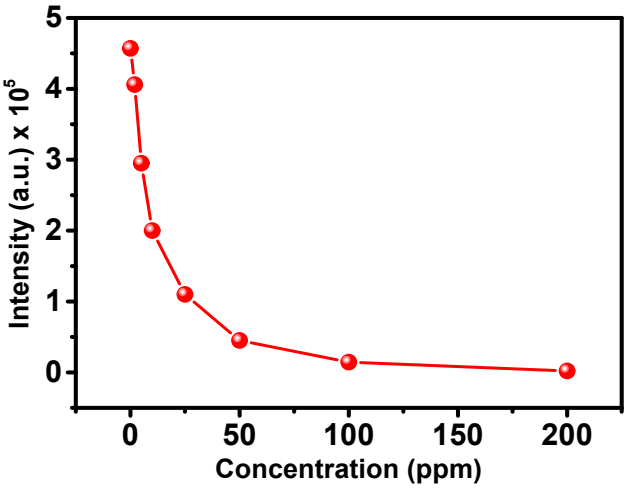

Fig. S27 Correlation between the luminescence intensity of **Zn-db-3** monitored at 575 nm and the concentration of CrO_4^{2-} ions.

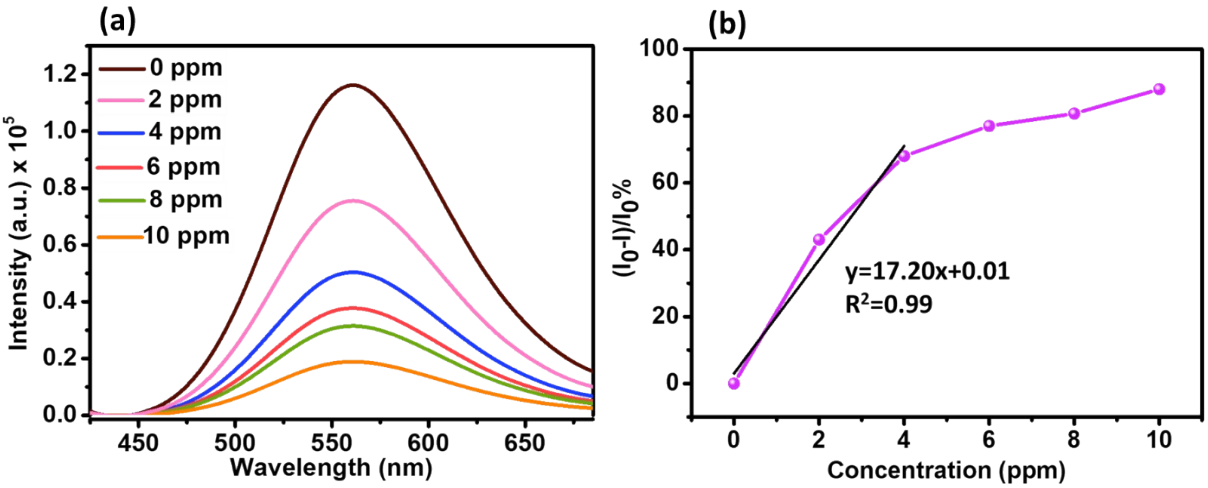

Fig. S28 (a) Luminescence spectra of **Zn-db-3** in CrO_4^{2-} deionized H_2O solutions with concentrations from 0 to 10 ppm. **(b)** Plot showing the quenching ratio of PL intensity (measured at 575 nm) of **Zn-db-3** as a function of the CrO_4^{2-} concentration.

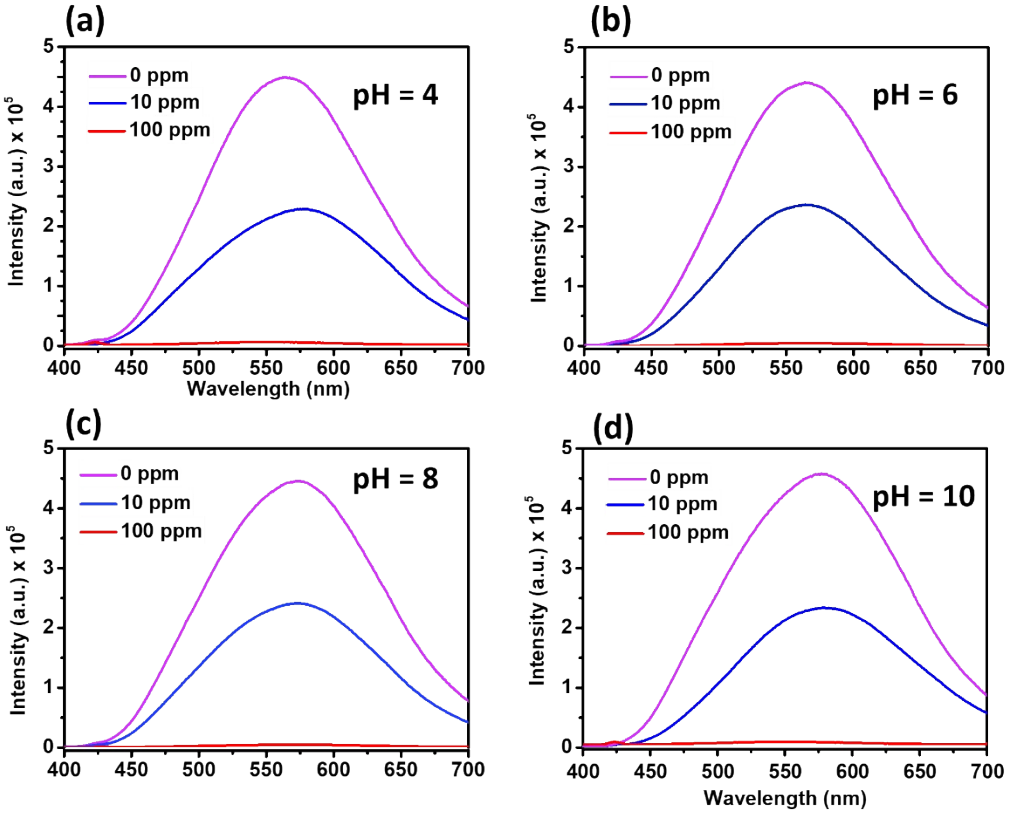

Fig. S29 CrO_4^{2-} sensing analysis by **Zn-db-3** monitored at different pH values (pH = 4,6,8, and 10).

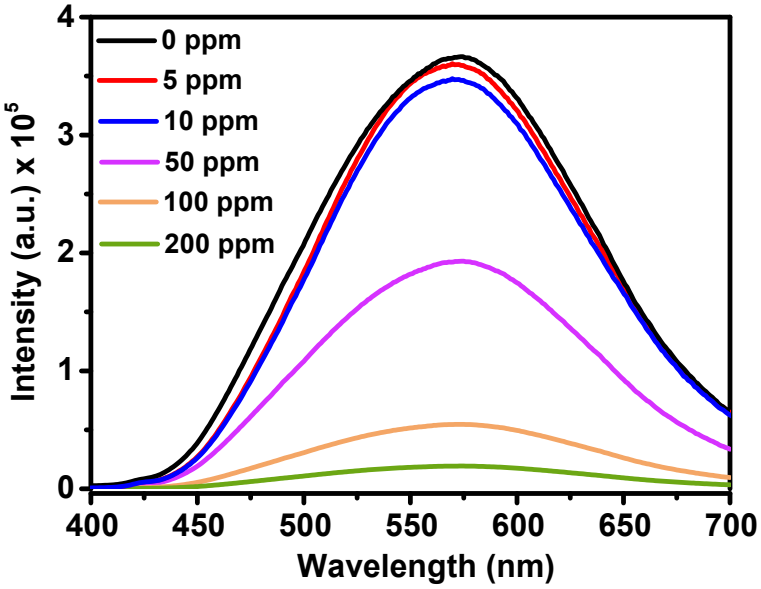

Fig. S30 Titration of an aqueous dispersion of **Zn-db** with CrO_4^{2-}.

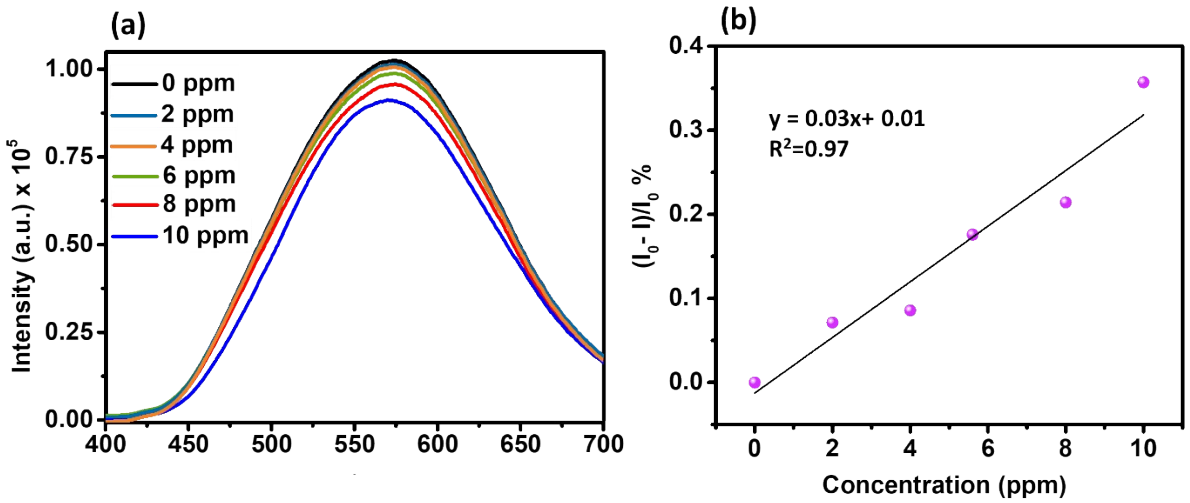

Fig. S31 (a) Luminescence spectra of **Zn-db** in CrO_4^{2-} deionized H_2O solutions with concentrations from 0 to 10 ppm. **(b)** Plot showing the quenching ratio of PL intensity (measured at 575 nm) of **Zn-db** as a function of the CrO_4^{2-} concentration.

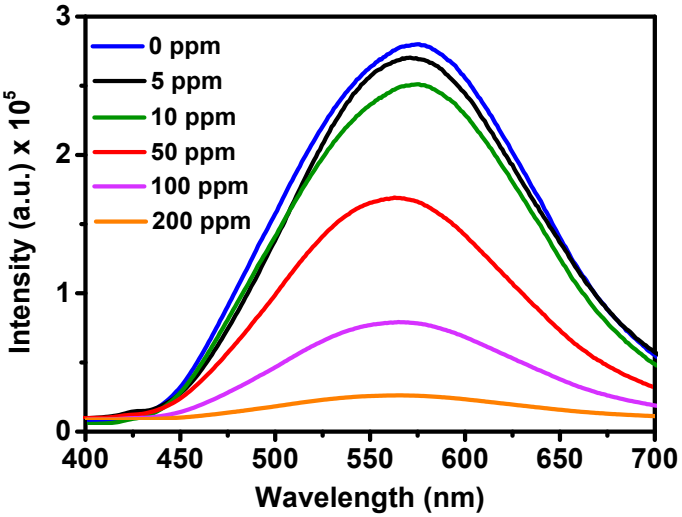

Fig. S32 Titration of a solution of **H_4DHT** in H_2O (0.5 mg/mL) with CrO_4^{2-}.

Table S8 Comparison of CrO_4^{2-} sensing performance of luminescent MOF materials

MOF	**LOD (ppb)**	**Detection Method**	**Response Time**	**Ref.**
$Cd_6(L)_2(bib)_2(DMA)_4$	-	Turn-off	300 s	15
$Cd_3(L)(bipy)_2$ $(DMA)_4$	-			
$Cd_3(L)(tib)(DMF)_2$	-			
$\{[Dy_2Zn(BPDC)_3(H_2O)_4](ClO_4)_2\cdot 10H_2O\}_n$	-	Turn-off	-	16
$[Zn(btz)]_n$	52	Turn-off	-	17
$[Zn_2(ttz)H_2O]_n$	104			
$[Eu_7(mtb)_5(H_2O)_{16}]\cdot NO_3\cdot 8DMA\cdot 18H_2O$	0.56	Turn-off	-	18
Zn-db-3	**12 ± 0.3**	**Shifted emission**	**< 30 s**	**This work**

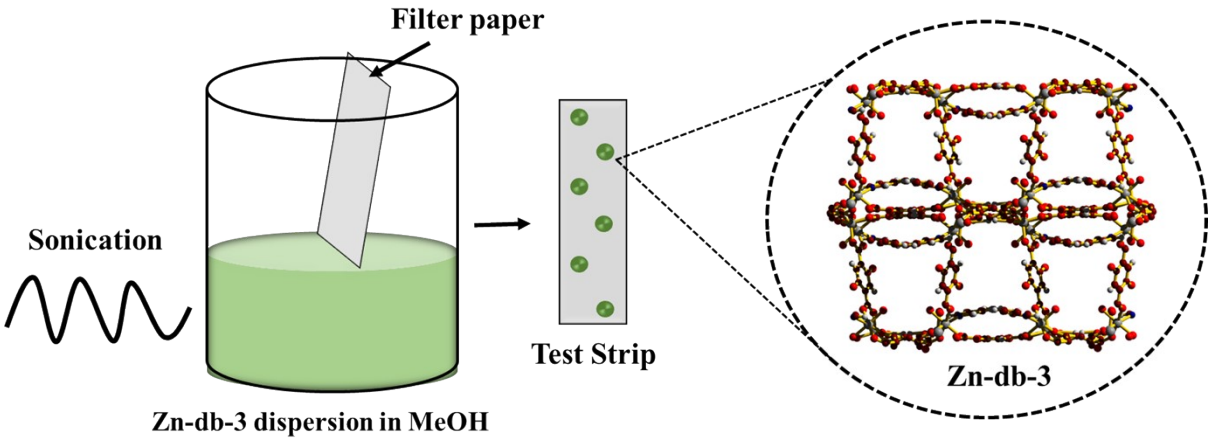

Fig. S33 Schematic for the fabrication of the luminescent test strip for the detection of CrO_4^{2-} ions.

References:

1. *SMART (V 5.628), SAINT (V 6.45a), Xprep, SHELXTL; Bruker AXS Inc. Madison, Wisconsin, USA*, 2004.
2. *G. M. Sheldrick, Siemens Area Detector Absorption Correction Program, University of Götingen, Götingen, Germany*, 1994.
3. A. Altomare, G. Cascarano, C. Giacovazzo, A. Guagliardi, M. C. Burla, G. Polidori and M. Camalli, *J. Appl. Crystallogr.*, 1994, **27**, 435-435.
4. *G. M. Sheldrick, SHELXL-97, Program for Crystal Structure Solution and Refinement, University of Götingen, Götingen, Germany*, 1997.
5. A. L. Spek, *J. Appl. Crystallogr.*, 2003, **36**.
6. *L. J. Farrugia, WinGX-A Windows Program for Crystal Structure Analysis, J. Appl. Crystallogr.*

, 1999, **32**.

7. L.-L. Wu, J. Zhao, H. Wang and J. Wang, *CrystEngComm*, 2016, **18**, 4268-4271.
8. J.-X. Wu and B. Yan, *Dalton Trans.*, 2017, **46**, 7098-7105.
9. S.-Y. Zhu and B. Yan, *Ind. Eng. Chem. Res.*, 2018, **57**, 16564-16571.
10. T. Wehner, K. Mandel, M. Schneider, G. Sextl and K. Müller-Buschbaum, *ACS Appl. Mater. Interfaces*, 2016, **8**, 5445-5452.
11. J. Othong, J. Boonmak, F. Kielar and S. Youngme, *ACS Appl. Mater. Interfaces*, 2020, **12**, 41776-41784.

12. L. Chen, J.-W. Ye, H.-P. Wang, M. Pan, S.-Y. Yin, Z.-W. Wei, L.-Y. Zhang, K. Wu, Y.-N. Fan and C.-Y. Su, *Nat. Commun.*, 2017, **8**, 15985.
13. A. Douvali, A. C. Tsipis, S. V. Eliseeva, S. Petoud, G. S. Papaefstathiou, C. D. Malliakas, I. Papadas, G. S. Armatas, I. Margiolaki, M. G. Kanatzidis, T. Lazarides and M. J. Manos, *Angew. Chem. Int. Ed.*, 2015, **54**, 1651-1656.
14. B. Li, W. Wang, Z. Hong, E.-S. M. El-Sayed and D. Yuan, *Chem. Commun.*, 2019, **55**, 6926-6929.
15. F.-Y. Yi, J.-P. Li, D. Wu and Z.-M. Sun, *Chem. Eur. J.*, 2015, **21**, 11475-11482.
16. P.-F. Shi, B. Zhao, G. Xiong, Y.-L. Hou and P. Cheng, *Chem. Commun.*, 2012, **48**, 8231-8233.
17. C.-S. Cao, H.-C. Hu, H. Xu, W.-Z. Qiao and B. Zhao, *CrystEngComm*, 2016, **18**, 4445-4451.
18. W. Liu, Y. Wang, Z. Bai, Y. Li, Y. Wang, L. Chen, L. Xu, J. Diwu, Z. Chai and S. Wang, *ACS Appl. Mater. Interfaces*, 2017, **9**, 16448-16457.